Proceedings of:
ASME TURBO EXPO 2000
May 8-11, 2000, Munich, Germany

2000-GT-0292

COMPUTED EFFECT OF RUB-GROOVE SIZE ON STEPPED LABYRINTH SEAL PERFORMANCE

David L. Rhode[1]
Mechanical Engineering Department
Texas A&M University
College Station, TX 77843

Richard G. Adams[2]
Texaco E & P, Inc.
400 Poydras Street
New Orleans, LA 70130

ABSTRACT

A numerical study was undertaken to explore the effects of the size of wear-in rub grooves that are typically cut into the abradable land of stepped labyrinth seals. The elliptic form of the 2-D axisymmetric Navier-Stokes equations for compressible turbulent flow were solved. The relationships among the friction coefficient, the leakage Reynolds number, the groove depth and width and the pre-rub radial clearance were examined.

It was found that the standard k-ε turbulence model and wall functions are effective for computing the friction coefficient and leakage for labyrinth seals with honeycomb land surfaces, both with and without the presence of rub grooves. The so-called rub grooves are the result of labyrinth teeth cutting wear grooves into the abradable surface of the land (stationary housing of the seal). Furthermore, it was found that the case of a small pre-rub tooth radial clearance, a wide rub groove and an intermediate step height is the most sensitive to the presence of a rub groove, with a leakage increase over the no-groove case of about 100 percent and 194 percent for the shallow and deep grooves, respectively. It was also found, for example, that the leakage varied with pre-rub clearance and groove width, in order from lowest to highest leakage, as: (a) small clearance and narrow groove, (b) small clearance and wide groove, (c) large clearance and narrow groove and (d) large clearance and wide groove.

INTRODUCTION

Energy consumption, for example, increases with increased seal leakage inside virtually all types of turbomachinery. Labyrinth seals have a widespread reputation for being very: (a) reliable, (b) able to perform well in harsh and "dirty" conditions and (c) forgiving under adverse conditions of, for example, extreme radial eccentricity, extreme axial displacement, extreme casing thermal distortion or out-of-roundness, extreme shaft run-out, etc. One reason for the high reliability and low cost of labyrinths is their simple design and fabrication, i.e. a single stationary ring around the rotor. Furthermore, because they have been used extensively since the early 1900s, both manufacturers and users have a high level of comfort with their low risk of causing the wide variety of problems experienced with other sealing alternatives.

An example of a rub groove in a stepped labyrinth seal can be seen in Figure 1. Although present in all turbomachinery testing, the effect of rub-grooves on abradable labyrinth leakage has rarely been investigated. That is, seal test rigs and the resulting semi-empirical labyrinth design models in current use have generally ignored these effects. Due to the need for advanced machines to operate at higher temperatures, tighter clearances, etc., more careful design understanding, analysis and methods are required. Rub grooves are the result of tight tooth radial clearances between the labyrinth teeth (knife blades on the rotor) and the land (i.e. the stator housing). The clearance changes substantially with wear and operating condition due to thermal and centrifugal radial growth, as well as thermal axial growth, for example. This causes a rub groove to be worn into the land that affects the performance of the seal. How the presence of the rub groove, as well as its dimensions, affects the seal leakage has remained relatively unexplored.

[1]Professor and Corresponding Author
[2]Graduate Research Assistant

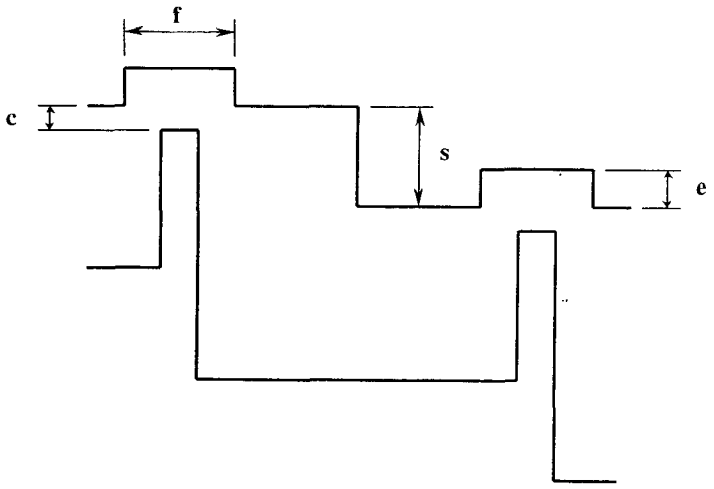

c = seal clearance, e = groove depth, f = groove width, and s = step height

FIGURE 1. THE GEOMETRIC PARAMETERS OF THE LABYRINTH STEPPED SEAL.

Labyrinths are used to satisfy different requirements such as: minimizing leakage; controlling the flow of coolant for thermal reliability; and preventing contaminants from entering a bearing chamber. Labyrinths work on the principle that the tooth-tip clearance converts fluid pressure energy into kinetic energy that is either dissipated into thermal energy or enters the subsequent tooth clearance as kinetic energy "carry-over".

The following section gives a review of the relevant literature. Then the objective is stated, which is followed by a summary of the numerical model. Next is a discussion of the findings from numerical testing of the use of the standard k-ε turbulence model and wall functions for a total of 37 measured cases of labyrinths, the majority of which had honeycomb lands with the presence of rub grooves. This is followed by a discussion of the results of computing generic stepped labyrinths with various generic groove sizes and pre-rub clearances, and the Summary.

NOMENCLATURE

c	pre-rub radial clearance, mm
C_D	discharge coefficient
C_μ	turbulence model constant
E	wall function constant
L	length of seal, mm
m	mass flow rate, kg/s
n	number of teeth in a labyrinth seal
P	pressure, MPa
R	radius, mm
Re	Reynolds number, 2Uc/ν
s	step height, mm
T	temperature, K
U	velocity in the x direction, m/s
V	velocity in the radial direction, m/s
V_r	wall tangent vector velocity, m/s
W	swirl velocity, m/s

Greek Characters

ε	specific turbulence energy dissipation, m^2/s^2
κ	von Karman constant
ρ	density, kg/m^3
μ	absolute viscosity, $N\text{-}s/m^2$
ν	kinematic viscosity, m^2/s
τ	shear stress, N/m^2

Subscripts

d	downstream
t	total
u	upstream
w	wall
r	radial direction
x	axial direction
θ	circumferential direction

PREVIOUS WORK

Stocker, et. al (1977) used static 2-D and rotating 3-D rigs to test various abradable materials and labyrinth geometries, and there were a few cases that included rub grooves. However, only the straight-through configurations with porous-abradable lands were tested with a rub groove present, and only one rub groove design was reported. The rub groove shape and size considered representative for their aircraft gas turbines was almost rectangular with a width of 0.6 mm (0.024 in) at the land surface and a depth of 0.25 mm (0.10 in.). They used three different tooth radial clearances of c = 0.13 mm (0.005 in), c = 0.25 mm (0.010 in) and c = 0.51 mm (0.020 in). Anomalous behavior was found in that the presence of grooves in the porous-abradable material frequently gave lower leakage than that with the non-grooved porous land. This unexpected finding is at least partially attributed to the fact that fabrication of the grooves appeared to close off the pores in the porous-abradable material. Thus the leakage was largely considered reduced by that portion of the leakage that would otherwise have passed through the pores. Thus it appears that the increased leakage associated with porous materials is significantly reduced in the presence of a grooved land. The 3-D test rig allowed them to test rub grooves that extend circumferentially over an azimuthal angle of 102° and of 360°. The 102° rub grooves simulate localized rub grooves due to eccentricities that have only worn away the stator over a given fraction of the entire circumference, whereas the 360° rub grooves simulate circumferential wear typically caused by rotor expansion and/or rotordynamic motion.

Zimmerman, Kammerer, and Wolff (1994) compared the results from a CFD model of a rub groove geometry involving a straight-through labyrinth as well as a stepped labyrinth geometry. Three fins were used in both cases. The study involved pre-rub clearances of 0.2 mm (0.008 in) and 0.4 mm (0.016 in.), and the groove was modeled as a rectangle of width 0.75 mm (0.030 in) and a depth of 0.2 mm (0.008 in). They found that for their operating conditions the rub grooves gave a very wide range of leakage increase.

Yu and Childs (1995) tested one labyrinth seal geometry at high pressure with teeth on the rotor and a grooved honeycomb stator. The experiment was designed to give rotordynamic force coefficients, and the test rig was excited horizontally to produce seal reaction forces. Air was used as the working fluid, and the shaft speed, inlet temperature, pressure distribution, and mass flow rate were all measured to determine the stiffness and damping coefficients. The shaft speed, pressure ratio, inlet pressure, and inlet swirl were all used as parameters for testing. As expected, a substantial increase in the shaft speed showed a small decrease in the mass flow rate of the seal. The inlet swirl conditions of no pre-swirl, intermediate pre-swirl, and high pre-swirl gave a minimal increase in the mass-flow rate as the pre-swirl increases.

Recently, flow visualization digital images of simulated rub grooves for straight-through labyrinths were obtained (Rhode and Allen, 1998). A very-large-scale, variable-geometry water visualization leakage test facility with unique variable-geometry and enlargement visualization capabilities was used. The digital images of glitter tracer particles were stored on the hard drive of a Pentium computer and later analyzed for an understanding of the throughflow jet trajectory effects on the leakage. The shape and size of the grooves investigated were chosen to encompass that considered by the scarce rub-groove data available from engine manufacturers (Stocker, et al, 1977 and Zimmermann, et al, 1994). The widths of the very-large-scale grooves investigated by Rhode and Allen (1998) were 8.128 cm (3.2 in.) and 16.26 cm (6.4 in.). The pre-rub tooth radial clearances (i.e. excluding the groove depth) were 0.635 cm (0.25 in.), 1.91 cm (0.75 in.) and 2.54 cm (1.0 in.). The single groove depth considered was 1.746 cm (0.688 in.). At larger radial clearances it was found that throughflow penetration into the rub groove alters the jet trajectory either toward the next tooth clearance (giving high kinetic energy carry-over) or away from it. In addition it was found that: (a) the leakage resistance (i.e. friction coefficient) is only slightly affected by rounded concave (i.e. groove bottom) corners versus sharp concave corners and (b) the leakage resistance decreases sharply with increasing groove depth.

The first visualization images of rub grooves in stepped labyrinths was also obtained using the above large-scale, variable-geometry water rig (Rhode and Allen, 1999). Fluorescein dye, activated by means of an Argon-ion laser, was used as the flow tracer for close-up rub groove movies, while glitter was used for (non-close-up) overall-view movies. The clearances and groove combinations used earlier for straight-through labyrinths (Rhode and Allen, 1998) were repeated for the stepped labyrinth investigation to allow proper comparisons of the important groove sizes. For the cases considered, the leakage resistance decrease due to the presence of the grooves for the large step height, for example, was 85 percent, 55 percent and 70 percent for the small, medium and large pre-rub clearances, respectively. Furthermore, a substantial tooth tip recirculation zone was observed, and its leakage significance was discussed.

The effect of shaft rotation on labyrinth seal leakage and heat transfer was investigated by, for example, Waschka, et al. (1990). Above a limiting leakage Re (= 2Uc/ν) of 5000 to 10000, the effect of shaft speed was found to be negligible. Other testing has shown an approximate 5 percent increase or decrease of leakage due to the presence of high shaft speed, depending on various details. Because most labyrinth applications operate with Re well above 10000, it is reasonable to state that labyrinth leakage is only slightly affected by shaft speed for realistic operating conditions.

Regarding new labyrinth configurations, Stocker, et al. (1975) utilized water flow visualization in the first phase of their labyrinth geometry investigation. The maximum performance for a given seal design concept was obtained by varying the clearance, tooth pitch and step height. The concept of increasing cavity turbulence to improve the leakage was confirmed. Furthermore, Rhode, et al. (1997a and 1997b) utilized the new flexibility of their very-large-scale, 2-D planar flow visualization/leakage test facility to study labyrinth configurations. The advantages of a new annular groove were explored, and leakage resistance increases over the baseline design of 26 percent were easily found. Other new configurations with far greater leakage improvements were found, but have not been reported thus far.

OBJECTIVE

Although the effects of rub grooves on seal leakage have typically been present in engine testing, very little quantitative understanding of them is available. This is particularly true for stepped labyrinth seals. Because of this lack of understanding, little progress toward developing improved empirical design models that can account for rub groove effects is possible. The present objective is to: (a) obtain an improved understanding of the effect of generic rub groove geometries on generic stepped labyrinths and (b) to determine the applicability of the wall function for honeycomb lands, both with and without rub grooves.

NUMERICAL MODEL

The solutions presented were obtained from a finite volume computer code that solves the complete compressible flow form of the steady, 2-D axisymmetric, elliptic Navier-Stokes equations for turbulent flow. The standard k-ε

turbulence model was used. Specifically, the equations were those for continuity; x-, r- and θ- momentum; stagnation enthalpy; and k and ε transport. These equations were solved using the well known SIMPLEC approach with the TDMA solution algorithm. Furthermore, the QUICK (Leonard, 1979) convection differencing scheme was utilized in order to reduce false diffusion, which can be important near the rub grooves considered here. This convective differencing scheme had previously been incorporated in a special way by Rhode, et al (1986) to promote numerical stability.

Because honeycomb material is often used as an abradable land, there is a modeling uncertainty to be determined in the present investigation which concerns the applicability of the wall function as a "boundary condition" along the abradable wall. Specifically, this uncertainty is due to the presence of the large number of exposed honeycomb cells, which give a different "apparent surface roughness" and potential for turbulence interaction between the cells and the through-flow. The standard wall function was used along all solid boundaries (stator land as well as the rotor surface) for the velocity components tangent to the wall, as well as for evaluating the turbulence production term in the turbulence energy equation, for which the standard formulation was used. The wall function was given by Launder and Spalding (1974) as

$$\frac{U}{(\tau/\rho)_w} C_\mu^{1/4} k^{1/2} = \frac{1}{\kappa} \ell n \left[Ey \frac{(C_\mu^{1/2} k)^{1/2}}{\nu} \right]. \qquad (1)$$

The turbulent wall stress τ is evaluated in terms of constants C_μ = 0.09, κ = 0.41 and E = 9.793 as well as the U, k and y values at the near wall grid point. The modification incorporated for the rotating surface is based on swirling pipe flow measurements of Backshall and Landis (1969), for example. It entails replacing the near-wall grid point value of U with the corresponding value $V_r = [U^2 + W^2]^{0.5}$ for walls parallel to the axial direction. The wall shear stress τ_t is then the vector sum of the axial and tangential components. These components, which are what actually enters into the computations, are then evaluated from $\tau_{r\theta} = \tau_t W/V_r$ and $\tau_{rx} = \tau_t U/V_r$. Walls parallel to the radial direction are treated similarly.

The seal leakage friction coefficient $1/C_D^2$ is an attractive parameter because it is easily related to previous work where the discharge coefficient was given. The discharge coefficient C_D was determined from the computed mass flow rate for a given pressure drop, and is defined as

$$C_D = \frac{\dot{m}}{\dot{m}_{ideal}} = \frac{\dot{m}}{\frac{P_{t,u} A}{\sqrt{T}} \sqrt{\frac{1-(P_{s,d}/P_{t,u})^2}{R(n + \ell n(P_{t,u}/P_{s,d}))}}} \qquad (2)$$

where n is the number of teeth of the labyrinth seal, $P_{t,u}$ is the total pressure upstream, and $P_{s,d}$ is the static downstream pressure. The assumptions used in the development of the ideal mass flow rate are that the flow is isothermal, there are many identical teeth and cavities with equal flow restrictions, there is complete conversion of kinetic energy to thermal energy in each cavity, and $P_{s,d}/P_{t,u} < 0.8$ (Egli, 1935).

Grid Independence

The results of the recent grid independence testing can be seen in Table 1. The table shows that the geometric configuration considered has the large pre-rub clearance, the deep- narrow groove and the intermediate step height. The leakage Reynolds number and the friction coefficient $1/C^2_D$ are both presented in the table for assessing grid independence. The percent difference given is the difference between that for a given grid and for the next finer grid, where the percent difference in the friction coefficient is defined as

$$\%Diff = \frac{\left| \left(\frac{1}{C_D^2} \right)_{finer-grid} - \left(\frac{1}{C_D^2} \right)_{coarser-grid} \right|}{\left(\frac{1}{C_D^2} \right)_{finer-grid}} \qquad (3)$$

In all production computer runs the intermediate grid was used because it shows less than a 3 percent difference from the next finer grid. These grids are non-uniform in both directions, each exhibiting several rates of expansion and contraction in order to resolve fine details economically. Grid stretching rates of between five percent and ten percent were typically used. Thus there is a much greater difference in grid spacing than the number of grid lines alone indicates. Furthermore, the near-wall grid spacing was maintained constant for these grids so that all of the y^+ values along the wall were within the proper range $12 < y^+ < 250$ for using wall functions. Specifically, most of the y^+ values were less than 100.

RESULTS

Wall Function Assessment For Abradable Lands

Honeycomb, and sometimes porous materials, are often used for abradable lands of gas turbine labyrinths. The degree of reliability of standard wall functions for computing the leakage and friction coefficient for such labyrinth lands has not been explored. Some types of porous material have a quite smooth surface texture, whereas honeycomb appears to offer a high level of apparent surface "roughness". Plotting the friction coefficient $1/C_D^2$ versus the leakage Reynolds number Re = U2c/ν allows for a convenient evaluation of the relative seal performance for the different configurations. Because the pre-rub radial clearance is extremely small compared to the shaft radius, the mass flow rate may be easily obtained from the

plotted values of Re, i.e. $m = (Re)(\pi D\mu/2)$. The $1/C_D^2$ quantity can be interpreted as a pressure loss quantity, i.e. as a leakage resistance friction coefficient.

The first two series of test cases were taken from the Stocker, et al (1977) experiment. They used a 2-D static (i.e. a slit between two plates) and also a 3-D rotating (i.e. wrapped around a shaft) test rig to study the effects on the leakage rate for labyrinth seals with four teeth and differing geometries and land materials. The difference in leakage measured using the 3-D rig and the 2-D rig for the same configuration and operating conditions was negligible. The 3-D test rig allowed for different shaft speeds of 0 rpm, 10,000 rpm, 20,000 rpm, and 30,000 rpm. The flow rate was determined using a standard ASME square orifice of 0.760 cm (0.299 in) diameter in a 4.925 cm (1.939 in) I.D. flow tube with static pipe taps for both the 2-D and 3-D test rigs.

The cases with a clearance of 0.25 mm (0.010 in), a tooth height of 2.03 mm (0.080 in), and a tooth pitch of 2.03 mm (0.080 in) were chosen. The inlet swirl component was estimated as 10 percent of the surface velocity of the shaft, and the reservoir temperature was estimated as 23 °C. Overall the model gave good predictions for the mass flow (i.e. Re) and the friction coefficient considering that only an average (over many tests) of the upstream pressure was available and that the experimental values had to be read from a figure.

For the first test case series, which consists of the non-grooved solid land cases (not shown for brevity), the deviation from measurements of the leakage mass flow at 10,000 rpm ranged from 1.6 percent underprediction to 6.9 percent underprediction. For the friction coefficient $1/C_D^2$ this translates to the range from 4.4 percent underprediction to 11.8 percent underprediction. Furthermore, the 20,000 rpm case gave nearly identical mass flow and friction coefficient deviation ranges to that at 10,000 rpm.

For the second test case series, Fig. 2(a) shows the comparison for the non-grooved honeycomb land of Stocker. The computational results are for the same operating conditions and rotor geometry as that of the non-abradable, solid land case above. The mass flow deviation from measurements varied from 9 percent overprediction to 6.8 percent underprediction for the 10,000 rpm case. The corresponding deviation values for the friction coefficient for the 10,000 rpm case had the range from 21 percent overprediction to 13 percent underprediction. Note that for the non-grooved solid land the curve for the predicted results has essentially the same shape and slope as that for the measurements. However, for the non-grooved honeycomb land, the predicted curve exhibits a slightly less positive slope at the higher Re. This is a result of the different surface roughness of each material.

For the third test case series, a labyrinth seal geometry with rub grooves in a honeycomb land was investigated. Specifically, the 27 Yu and Childs (1995) cases with a rub-groove were computed over a wide range of Re. The Yu and Childs (1995) experiment was designed to obtain the rotordynamic coefficients for an eleven-tooth labyrinth seal with a rub-grooved stator.

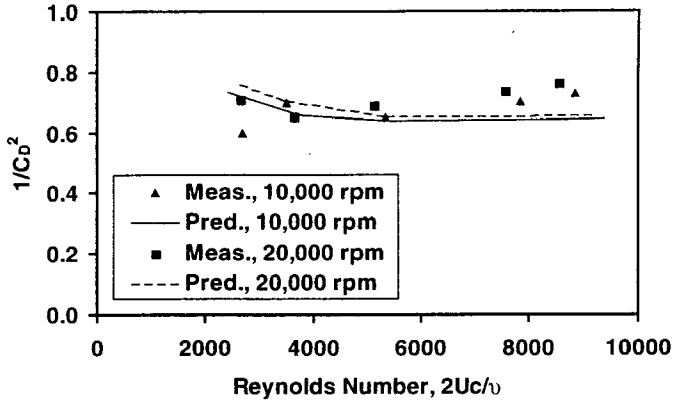

(a) Non-Grooved Honeycomb Land

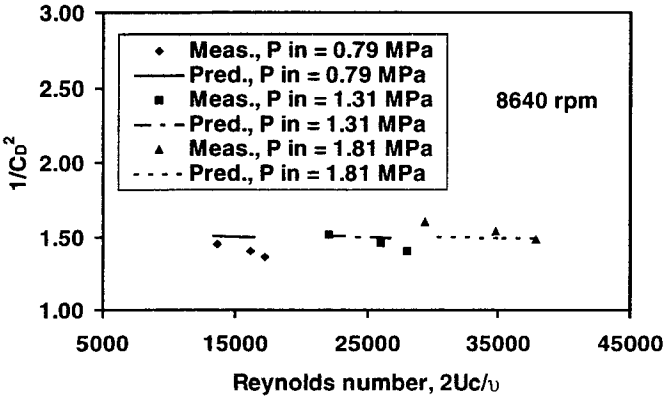

(b) Grooved Honeycomb Land

FIGURE 2. COMPARISON BETWEEN THE PREDICTIONS AND THE MEASUREMENTS OF: (A) STOCKER, ET AL. (1997) AND (B) YU AND CHILDS (1995).

The test rig was excited horizontally to create dynamic seal forces so that the stiffness and damping force coefficients could be determined. For this reason the groove width was 2.06 mm (0.081 in), which was about half the tooth pitch of 4.14 mm (0.163 in). The groove depth was 0.152 mm (0.006 in) with a pre-rub clearance of c = 0.152 mm (0.006 in). In order to allow all 27 of the grooved honeycomb measured cases to be computed, the computational domain was reduced from ten cavities to three cavities, and the fourth cavity measurement of the pressure was used as the downstream pressure. No other geometry approximations were made, and the in-situ measured pre-rub radial clearance was used in the present computation.

Figure 2(b) shows the comparison of the numerical prediction with the experimental results for a much wider range

of Re and a shaft speed of 8640 rpm. This figure shows that the maximum deviation for the mass flow at the lowest P_{in} value is approximately 5.2 percent overpredicted, whereas for the highest P_{in} value it is approximately 3.2 percent underpredicted. Furthermore, the maximum deviation for the friction coefficient for the lowest P_{in} was 11 percent overpredicted, whereas for the highest P_{in} it was 6.3 percent underpredicted. However, in Figure 2(b) the numerical prediction shows a curve of somewhat smaller slope than that measured.

In addition, the average deviation for the mass flow rate was 5.1 percent for the entire set of 27 Yu and Childs grooved honeycomb cases. Considering the approximation of computing only three cavities, it is concluded that the use of the standard wall function and k-ε model is effective for accurately computing the leakage and friction coefficient for a labyrinth seal with rub grooves in a honeycomb land.

Rub Groove Size Effects

The fluid properties remain essentially constant from case to case because the upstream and downstream reservoir pressures and the upstream temperature are held fixed. With fixed fluid properties and pre-rub tooth radial clearance, an increase in the leakage Reynolds number indicates an increase in the velocity and thus in the mass flow rate. The numerical results for Reynolds numbers less than 8,000 were not expected to be particularly accurate because the standard k-ε turbulence model is based on high Reynolds number assumptions. However, Figure 2(a) shows a comparison of the numerical results and the Stocker, et al. (1977) measurements for some lower Reynolds numbers, and the model gave accurate results.

The Cases Considered. The shape of the grooves considered here was chosen to be somewhat representative of abradable labyrinths found in many sizes of gas turbine engines. Unfortunately this is difficult to establish because of the extremely wide range of gas turbines extending from missile engines to large power generation machines. It was learned that a very wide range of groove shapes have been observed in refurbishment operations, some of which had rounded corners and others non-rounded corners. This range apparently depended on the extent of the axial and radial transient thermal growth of the rotor relative to the stator, the rotor radial centrifugal growth, the accumulation of manufacturing tolerances, etc. Furthermore, it had recently been determined experimentally that the shape of a generic groove is of little importance. Specifically, the two limiting cases of groove shape, i.e. a rectangular groove as well as a completely rounded groove, had been compared in a large scale test facility (Rhode and Allen, 1999) where the planned experiments of the rounded groove were discontinued. The reason the rounded shape was discontinued is that it gave only slightly decreased leakage over that of the rectangular groove, and this occurred only for a certain range of Re.

The dimensions of the rectangular groove shape considered here were selected to encompass that chosen in studies by gas turbine manufacturers, i.e. that by Zimmermann, et al (1994) and by Stocker, et al (1977). The variable dimensions of the present seal designs are defined in Fig. 1. Three different step heights of s = 0.406 mm (0.016 in), s = 0.813 mm (0.032 in), and s = 1.626 mm (0.064 in) were chosen for the numerical predictions. Furthermore, the "small" tooth radial clearance of c = 0.102 mm (0.004 in) and the "large" clearance of c = 0.203 mm (0.008 in) were considered as well as the "narrow" and "wide" grooves of f = 0.762 mm (0.030 in) and f = 1.524 mm (0.060 in), respectively. In addition, the no-groove case of e = 0.0 mm, the "shallow" groove case of e = 0.102 mm (0.004 in), and the "deep" groove case of e = 0.203 mm (0.008 in) were compared.

Discussion. The expression for obtaining the mass flow rate from the plotted leakage Re is given above (see Wall Function Assessment for Abradable Lands). Compared to straight-through labyrinths, stepped labyrinths create a more serpentine throughflow pattern by deflecting the throughflow jet from a straight-line path with a series of steps. The presence of a rub groove adds complexity to the flow pattern. Figure 3 presents the leakage results for the "large" pre-rub clearance of c = 0.203 mm (0.008 in.) and the "wide" groove of f = 1.52 mm (0.06 in.). The presence of either of the two rub grooves considered causes a substantial increase in the leakage Reynolds number and a decrease in the friction coefficient. Furthermore, the leakage Reynolds number for the no-groove case shows little dependence on the step height. However, the grooved cases do show a substantial step height dependence, especially for the deep groove of e = 0.203 mm (0.008 in.). Specifically, the leakage Reynolds number increases by about 44 percent and 97 percent upon adding the shallow e = 0.102 mm groove and the deep e = 0.203 mm groove, respectively, for the intermediate step height, for example. Also, the small step has the highest leakage rate for both grooved cases. It is interesting that the variation of $1/C_D^2$ with step height is about the same for the groove depth of 0 mm and 0.203 mm, but the variation of leakage (i.e. Re) increases significantly with this change of groove depth. This is a reflection of the fact that, for a given pre-rub clearance, as the effective tooth-clearance area (i.e. groove depth) increases, the step height has a more significant effect on the throughflow pattern. Furthermore, as the effective tooth-clearance area increases, the leakage rate as well as Re increase, which intensifies the turbulence and gives the well known asymptotic Re independence behavior similar to pipe flow turbulent friction.

The increased leakage due to an increase in the effective tooth-tip flow area is seen in the velocity vectors of Figures 4 and 5 for the small step height case. Figure 4 gives the velocity vectors for the no-groove case, and the longer

vectors of Figure 5 illustrate the increase in leakage for the "wide-deep" (wide and deep) groove. The effective leakage area is proportional to the distance H-I in the figures.

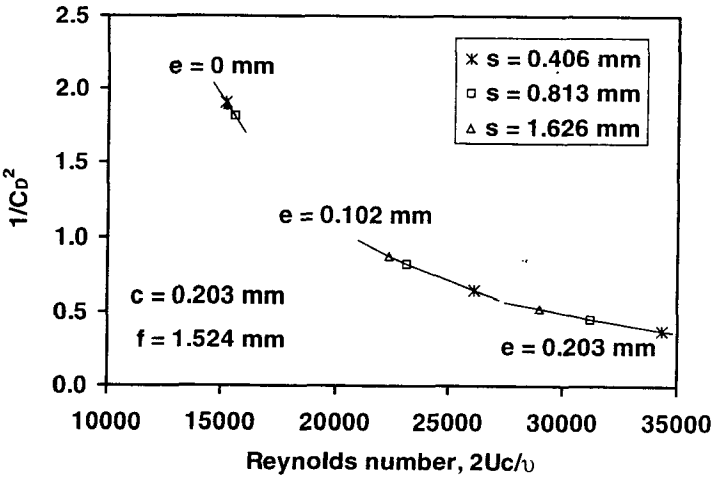

FIGURE 3. FRICTION COEFFICIENT VERSUS REYNOLDS NUMBER FOR A STEPPED LABYRINTH SEAL (WIDE RUB GROOVES, LARGE CLEARANCE).

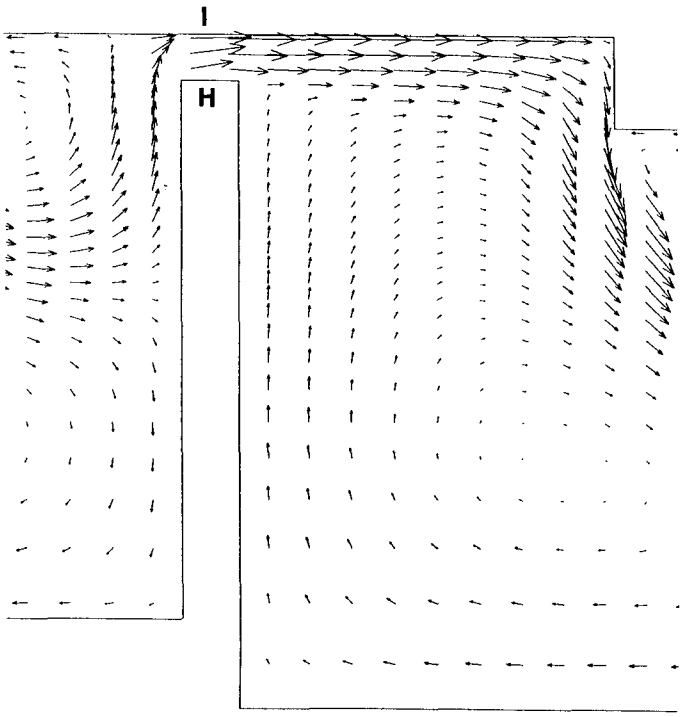

c = 0.203 mm, e = 0 mm, f = 0 mm, s = 0.406 mm

FIGURE 4. AN ENLARGED VIEW OF THE VELOCITY VECTORS FOR A STEPPED LABYRINTH (NO RUB GROOVES, LARGE CLEARANCE, SMALL STEP HEIGHT).

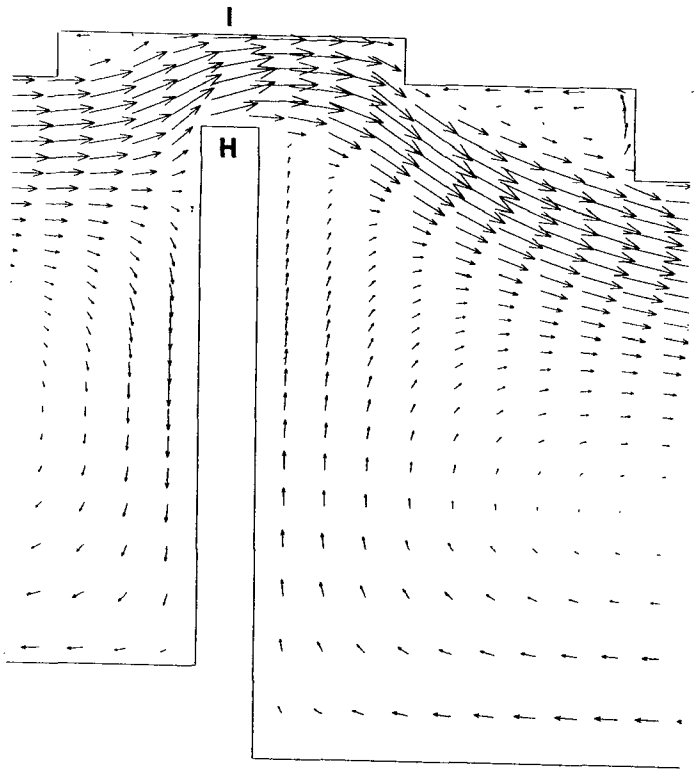

c = 0.203 mm, e = 0.203, f = 1.524 mm, s = 0.406 mm

FIGURE 5. AN ENLARGED VIEW OF THE VELOCITY VECTORS FOR A STEPPED LABYRINTH (WIDE RUB GROOVES, LARGE CLEARANCE, SMALL STEP HEIGHT).

The change in overall flow pattern can be seen more clearly in Figures 6 and 7, which are for the same cases presented in Figures 4 and 5, respectively, but now with the overall view instead of the enlarged view. The throughflow for the no-groove case in Fig. 6 is deflected by the step, but the presence of the rub groove diverts the flow past the step as shown in Figure 7. The increase in the width and velocity of the throughflow jet of the grooved case clearly indicates the increased leakage of this case. The rub groove limits the serpentine flow character of the stepped geometry.

The effect of the step height on the overall flow pattern is seen by comparing the large step cases of Figures 8 and 9, with the corresponding ones for the smallest step in Figs. 6 and 7. The flow is completely deflected by the step for the no-groove case, and since the step height is much larger here, the flow is also substantially deflected in the rub groove case.

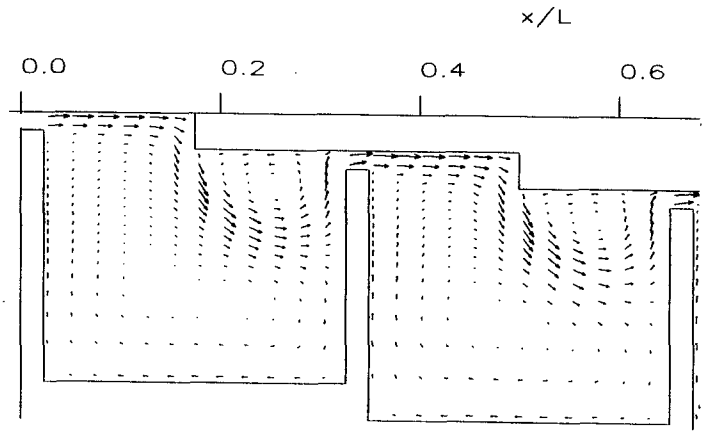

c = 0.203 mm, e = 0 mm, f = 0 mm, s = 0.406 mm

FIGURE 6. VELOCITY VECTORS FOR A THREE-CAVITY STEPPED LABYRINTH (NO RUB GROOVES, LARGE CLEARANCE, SMALL STEP HEIGHT).

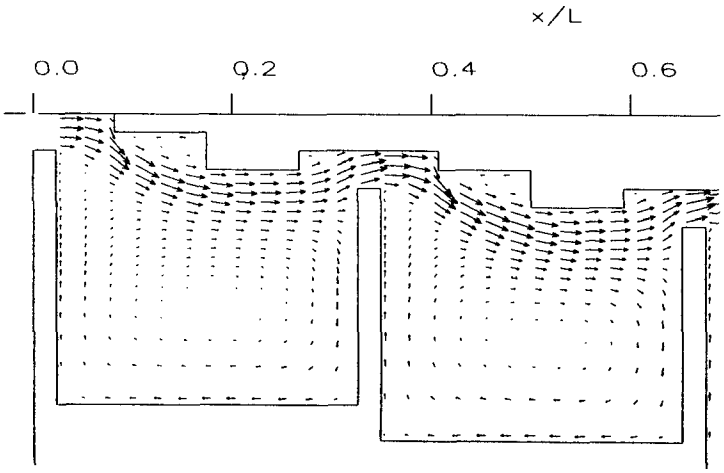

c = 0.203 mm, e = 0.203 mm, f = 1.524 mm, s = 0.406 mm

FIGURE 7. VELOCITY VECTORS FOR A THREE-CAVITY STEPPED LABYRINTH (WIDE RUB GROOVES, LARGE CLEARANCE, SMALL STEP HEIGHT).

The large step makes the throughflow trajectory similar for both cases; however the leakage is still increased due to the presence of the rub groove, but not as severely as for the small step height.

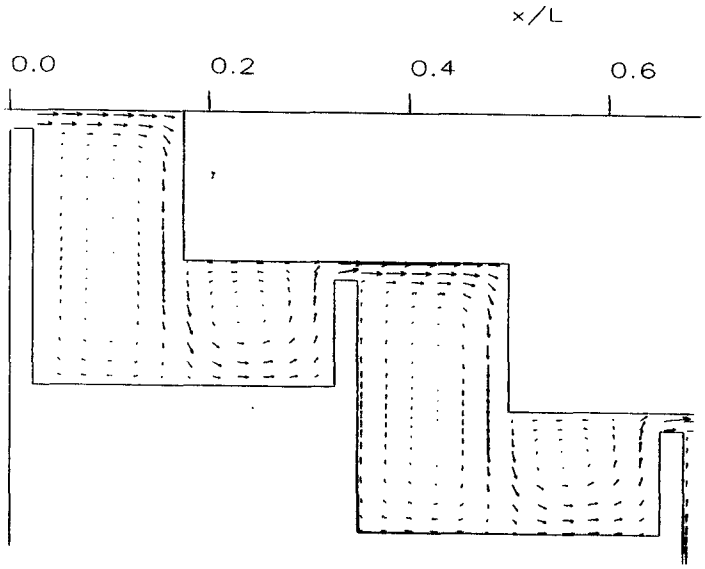

c = 0.203 mm, e = 0 mm, f = 0 mm, s = 1.626 mm

FIGURE 8. VELOCITY VECTORS FOR A THREE-CAVITY STEPPED LABYRINTH (NO RUB GROOVES, LARGE CLEARANCE, LARGE STEP HEIGHT).

The effect of the narrow groove [f = 0.762 mm (0.03 in.)] with the large clearance c = 0.203 mm (0.008 in.) is shown in Figure10 where the seal geometry is otherwise the same as that of Figure 3. Compared to Fig. 3 there is less variation of leakage with step height and groove depth. However, there is still a significant difference between the no-groove cases and the corresponding grooved cases. Specifically, the leakage is seen to increase by about 39 percent and 51 percent, for example, upon adding the shallow [e = 0.102 mm (0.004 in.)] and the deep [0.203 mm (0.008 in.)] grooves, respectively, for the intermediate step height case of Fig. 10. Thus the presence of the narrow-shallow groove gives a slightly smaller leakage increase (about 39 percent in Fig. 10) than does the presence of the wide-shallow groove (about 44 percent in Fig. 3). However, the presence of the narrow-deep groove gives substantially less leakage increase (abut 51 percent in Fig. 10 versus about 97 percent in Fig. 3) than does the wide-deep groove. The better performance of the narrow-shallow and narrow-deep grooves is a result of the small flow constriction H-J which is seen to be dominant over the H-I constriction in Fig. 11 for the intermediate step height. Figure 12 shows the corresponding wide groove case which is an example where the H-I constriction dominates, and the H-J constriction has little effect. Thus the smaller effective tooth-clearance area of the narrow-deep groove accounts for the fact that it has, for example, 25 percent lower leakage (Fig. 10) than does the corresponding wide groove (Fig. 3) for the intermediate step height.

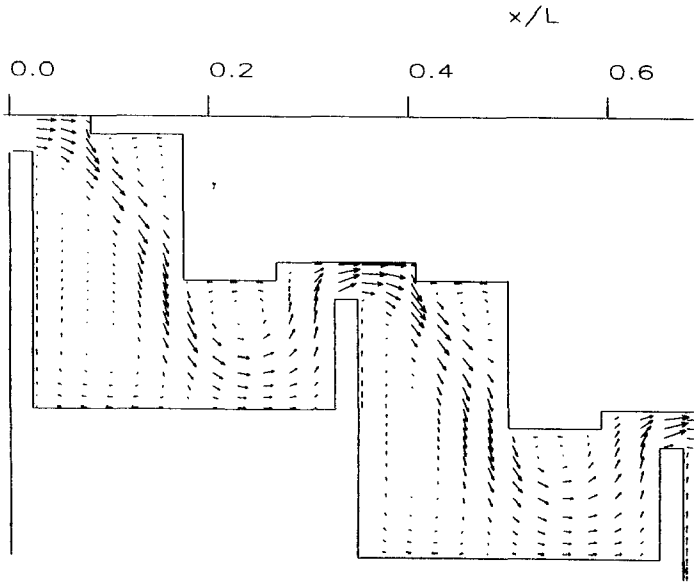

c = 0.203 mm, e = 0.203 mm, f = 1.524 mm, s = 1.626 mm

FIGURE 9. VELOCITY VECTORS FOR A THREE-CAVITY STEPPED LABYRINTH (WIDE RUB GROOVES, LARGE CLEARANCE, LARGE STEP HEIGHT).

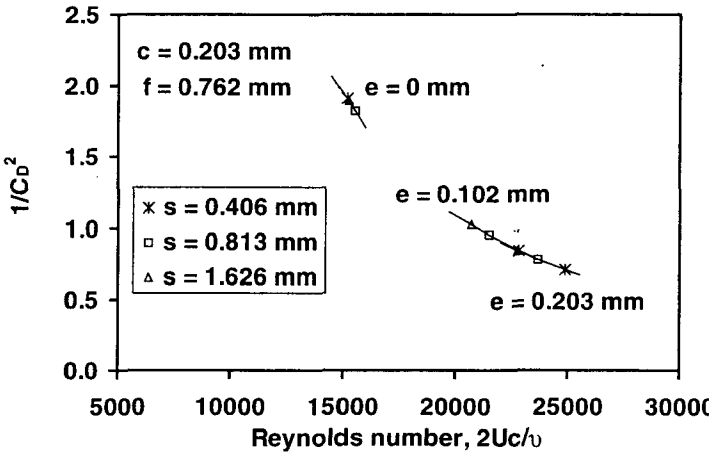

FIGURE 10. FRICTION COEFFICIENT VERSUS REYNOLDS NUMBER FOR A STEPPED LABYRINTH (NARROW RUB GROOVES, LARGE CLEARANCE).

The overall view of the velocity vectors, for the geometry of Figures 11 and 12 is shown in Figure 13 which considers the narrow-deep groove. The overall view for the corresponding wide-deep groove is nearly the same, and is therefore omitted for brevity. Furthermore, comparison of Figures 3 and 10 reveals that reducing the groove width for the case of small groove depth does not give as much leakage reduction as it does for the case of large groove depth. That is, for the small groove depth, the H-J constriction is not as significant as for the large depth. This explains why Figures 3 and 10 show that, for the shallow groove cases, the narrow groove exhibits only about 7 percent less leakage than does the wide groove, for the intermediate step height. The velocity vectors for the shallow-narrow groove and for the shallow-wide groove are omitted because they are also almost the same as that of Fig. 13. Furthermore, the flow exiting a tooth clearance has less of a downward trajectory than for the large groove depths, and thus the throughflow jet is deflected more by the presence of the step for the shallow groove cases.

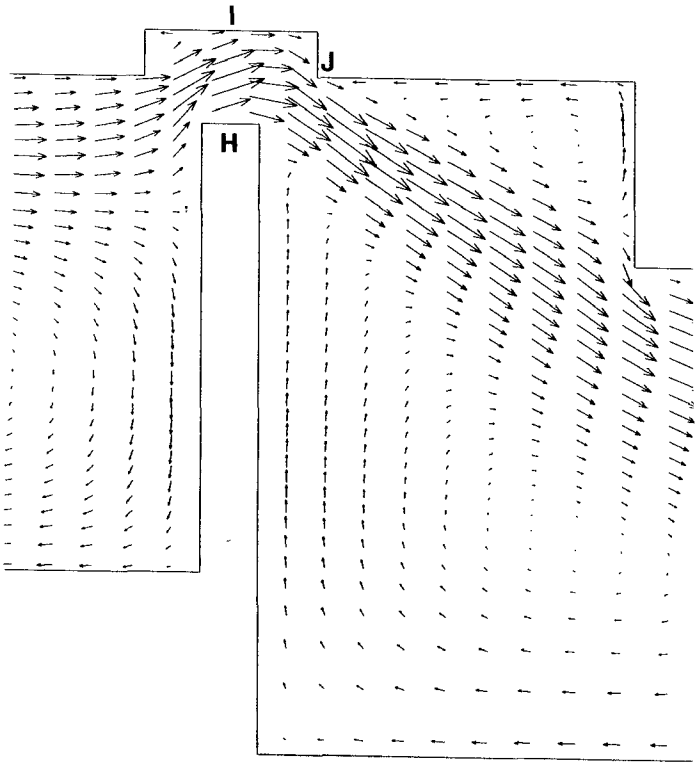

c = 0.203 mm, e= 0.203 mm, f = 0.762 mm, s = 0.813 mm

FIGURE 11. AN ENLARGED VIEW OF THE VELOCITY VECTORS FOR A STEPPED LABYRINTH (NARROW RUB GROOVES, LARGE CLEARANCE, MEDIUM STEP HEIGHT).

The results are shown in Figure 14 for the cases with small clearance and wide grooves. Here there is even less dependence on step height than previously, but there is a very large dependence on groove depth. Specifically, the leakage increases by about 100 percent and by 194 percent due to the presence of the shallow-wide and deep-wide grooves, respectively. Furthermore, comparing Fig. 14 with the corresponding large clearance data of Fig. 3, one finds the

expected result that the small clearance generally gives much lower leakage for all cases considered.

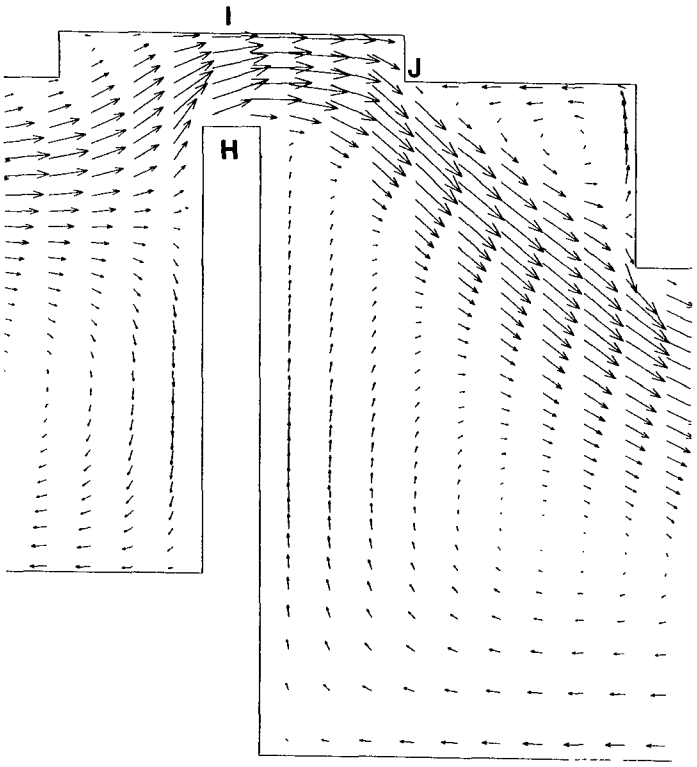

c = 0.203 mm, e = 0.203 mm, f = 1.524 mm, s = 0.813 mm

FIGURE 12. AN ENLARGED VIEW OF THE VELOCITY VECTORS FOR A STEPPED LABYRINTH (WIDE RUB GROOVES, LARGE CLEARANCE, MEDIUM STEP HEIGHT).

However, the small clearance cases give a leakage reduction from the corresponding large clearance cases (wide groove) of 50 percent, 30 percent and 25 percent for the groove depth e = 0 mm, 0.102 mm (0.004 in.) and 0.203 mm (0.008 in.), respectively.

The small clearance and narrow groove cases of Figure 15 indicate that the leakage increases by about 88 percent and 125 percent due to the presence of the shallow and deep grooves for the intermediate step height, respectively. In addition, this figure shows even less dependence on step height than previously found, especially for the deep groove cases. The small step height is four times the clearance and severely deflects the throughflow radially inward. However, for the large clearance, the small step height is only twice the clearance, and the flow is not severely deflected as is shown in Figure 6. The vector plot for the narrow-deep, small clearance and large step case is given in Figure 16. The large clearance version of the same geometry gives an almost identical flow pattern and is thus omitted.

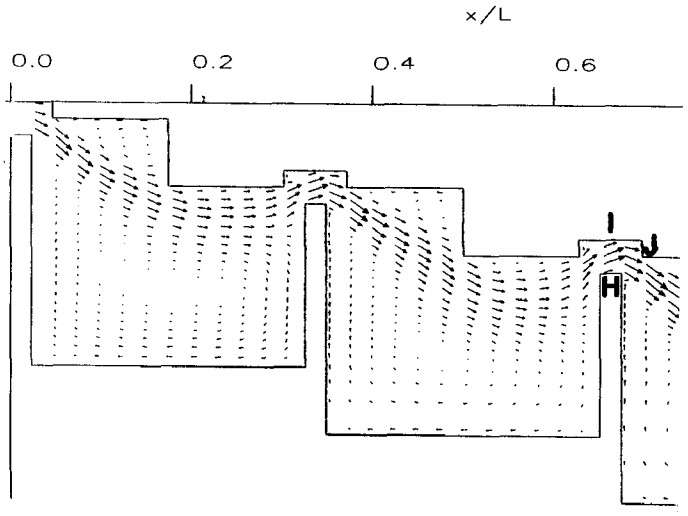

c = 0.203 mm, e = 0.203 mm, f = 0.762 mm, s = 0.813 mm

FIGURE 13. VELOCITY VECTORS FOR A THREE-CAVITY STEPPED LABYRINTH (NARROW RUB GROOVES, LARGE CLEARANCE, MEDIUM STEP HEIGHT).

However, the velocity vectors of the large clearance case are longer, indicating higher velocity and increased leakage. Furthermore, there is little difference in flow pattern between the small clearance and small step height case of the figure, and the corresponding large clearance and small step height case, which is also omitted.

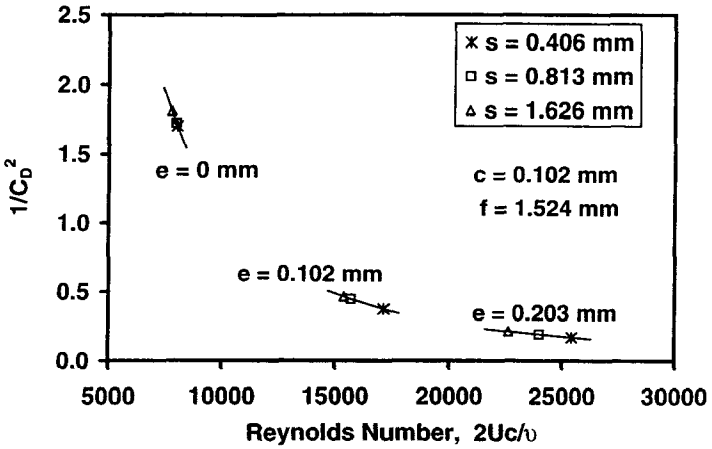

FIGURE 14. FRICTION COEFFICIENT VERSUS REYNOLDS NUMBER FOR A STEPPED LABYRINTH (WIDE RUB GROOVES, SMALL CLEARANCE).

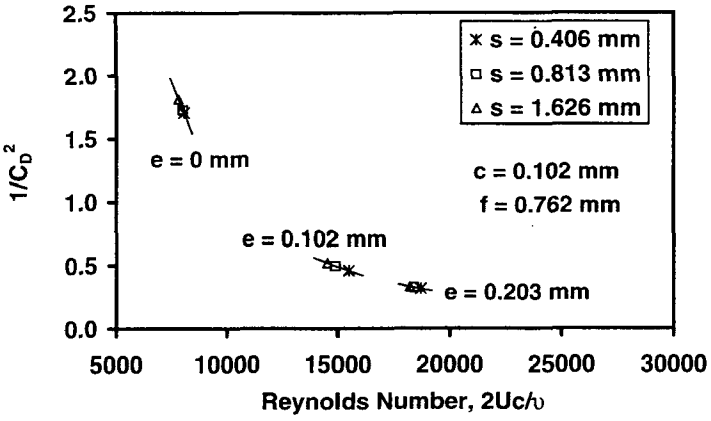

FIGURE 15. FRICTION COEFFICIENT VERSUS REYNOLDS NUMBER FOR A STEPPED LABYRINTH (NARROW RUB GROOVES, SMALL CLEARANCE).

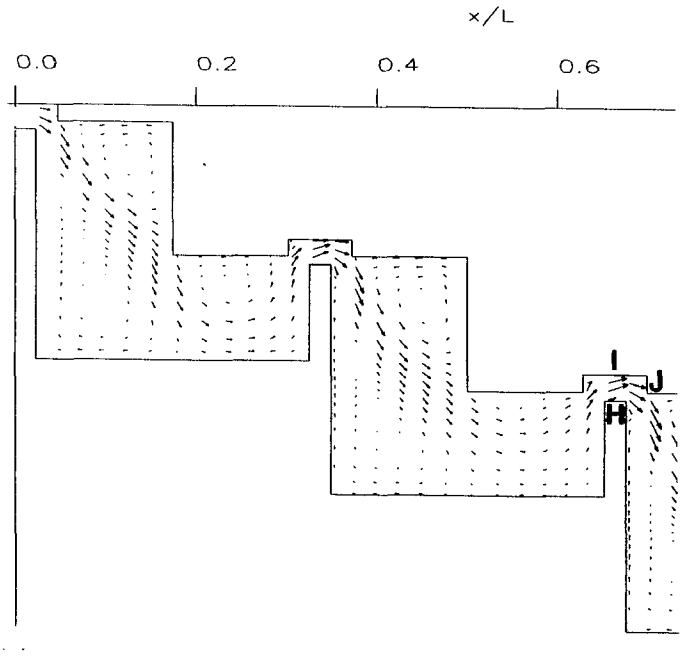

c = 0.102 mm, e = 0.203 mm, f = 0.762 mm, s = 1.626 mm

FIGURE 16. VELOCITY VECTORS FOR A THREE-CAVITY STEPPED LABYRINTH (NARROW RUB GROOVES, SMALL CLEARANCE, LARGE STEP HEIGHT).

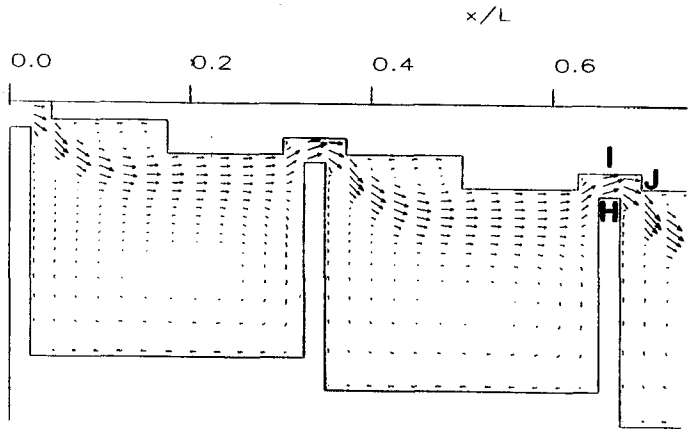

c = 0.102 mm, e = 0.203 mm, f = 0.762 mm, s = 0.406 mm

FIGURE 17. VELOCITY VECTORS FOR A THREE-CAVITY STEPPED LABYRINTH (NARROW RUB GROOVES, SMALL CLEARANCE, SMALL STEP HEIGHT).

SUMMARY

It has been determined that the use of the high-Re k-ε model with wall functions is effective for computing the leakage and friction coefficient for labyrinths with a honeycomb land, both with and without rub grooves. It was also shown how, for gas labyrinths with steps, the increase in the effective tooth-clearance flow area from the presence of a rub groove gives a large increase in leakage. Furthermore, the cause-and-effect relationship was explored between the size of the rub groove and the resulting increase of leakage. Some specific findings include:

1. A deeper groove gives increased leakage; this is primarily attributed to: (a) an increased effective tooth clearance area and (b) altered energy losses due to the altered throughflow pattern due to the presence of the groove.

2. For the shallow groove and intermediate step, for example, the leakage varied with pre-rub clearance and groove width, in order from lowest to highest leakage, as: (a) small clearance and narrow groove, (b) small clearance and wide groove, (c) large clearance and narrow groove and (d) large clearance and wide groove.

3. The case of small clearance, wide groove and intermediate step is the most sensitive to the presence of a groove, with leakage increases over the no-groove case of about 100 percent and 194 percent for the shallow and deep grooves, respectively.

4. For the narrow groove, the advantage of the large step height was negated, but for the wide groove it was not negated due to through flow pattern effects.

5. It is interesting to note that the variation of $1/C_D^2$ with step height is about the same for the change of groove depth from 0 mm to 0.203 mm, but the variation of leakage (i.e. Re) increases significantly with increasing groove depth.

This is a reflection of the fact that, for a given pre-rub clearance, as the effective tooth-clearance area (i.e. groove depth) increases, the step height has a more significant effect on throughflow pattern and the resulting energy loss mechanism.

ACKNOWLEDGMENTS

The authors are grateful for the financial support of the Texas ATP and the NASA CSP. Also, they are indebted to the Supercomputer Center of Texas A & M University for large grants of computer resources.

Table 1 Grid Independence Testing
c = 0.203 mm, e = 0.203 mm, f = 0.762 mm, s = 0.813 mm.

Grid Size	Reynolds Number	% Difference	$1/C^2_D$	% Difference
96x83	24,575	3.85%	2.905	6.83%
122x108	23,663	1.39%	3.118	2.71%
162x144	23,339	-	3.205	-

REFERENCES

Backshall, R.G. and Landis, F., 1969, "The Boundary-Layer Velocity Distribution in Turbulnet Swirling Pipe Flow," *ASME Jl. Of Basic Engineering*, Vol. 91, pp. 728 - 733.

Egli, A., 1935, "The Leakage of Steam Through Labyrinth Seals," *ASME Transactions Journal of Fuels and Steam Power,* Vol. 57, pp. 115-122.

Launder, B.E. and Spalding, D.B., 1974, "The Numerical Computation of Turbulent Flows," *Computer Methods in Applied Mechanics and Engineering*, Vol. 3, pp. 269 - 289.

Leonard, B.P., 1979, "A Stable and Accurate Convective Modeling Procedure Based on Quadratic Upstream Interpolation," *Computer Methods in Applied Mechanics and Engineering,* vol. 19, pp. 59-98.

Rhode, D.L. and Allen, B.F., 1999, "Measurement and Visualization of Leakage Effects of Rounded Teeth Tips and Rub-Grooves on Stepped Labyrinths", ASME paper 99-GT-377, presented at the ASME International Gas Turbine & Aeroengine Congress & Exhibition, Indianapolis; also accepted for the ASME *Journal of Turbomachinery.*

Rhode, D.L. and Allen, B.F., 1998, "Visualization and Measurements of Rub-Groove Leakage Effects on Straight-Through Labyrinth Seals", ASME paper 98-GT-506, presented at the ASME International Gas Turbine & Aeroengine Congress & Exhibition, Stockholm.

Rhode, D.L., Johnson, J.W. and Broussard, D.H., 1997a, "Flow Visualization and Leakage Measurements of Stepped Labyrinth Seals; Part 1: Annular Groove," *ASME Jl. of Turbomachinery*, Vol. 119, pp. 839 - 843.

Rhode, D.L., Younger, J.S. and Wernig, M.D., 1997b, "Flow Visualization and Leakage Measurements of Stepped Labyrinth Seals; Part 2: Sloping Surfaces," *ASME Jl. of Turbomachinery*, Vol. 119, pp. 844 -848.

Rhode, D.L., Demko, J.A., Traegner, U.K., Morrison, G.L., and Sobolik, S.R., 1986, "Predictions of Incompressible Flow in Labyrinth Seals," *ASME Journal of Fluids Engineering,* vol. 108, pp. 19-25.

Rhode, D.L. and Sobolik, S.R., 1986, "Simulation of Subsonic Flow through a Generic Labyrinth Seal," *ASME Journal of Engineering for Gas Turbines and Power,* vol. 108, pp. 674-680.

Stocker, H.L., 1975, "Advanced Labyrinth Seal Design Performance for High Pressure Ratio Gas Turbines," ASME Paper 75-WA/GT-22.

Stocker, H.L., Cox, D.M., and Holle, G.F, 1977, "Aerodynamic Performance of Conventional and Advanced Design Labyrinth Seals with Solid-Smooth, Abradable, and Honeycomb Lands," NASA Contract Report NAS 3-20056.

Yu, Z. and Childs, D.W., 1995, "Experimental Rotordynamic Coefficient and Static Characteristic Results for a Labyrinth Rotor Running Against a Grooved Stator with L/D = 0.466, C_r/r = 0.0036," Turbomachinery Laboratories Report, Texas A&M University.

Waschka, W., Wittig, S. and Kim, S., 1992, "Influence of High Rotational Speeds on the Heat Transfer and Discharge Coefficients in Labyrinth Seals," *ASME Jl. of Turbomachinery*, Vol. 114, pp. 462 - 468.

Zimmerman, H., Kammerer, A. and Wolff, K.H., 1994, "Performance of Worn Labyrinth Seals," paper ASME 94-GT-131, presented at the International Gas Turbine and Aeroengine Congress and Exposition, The Hague, Netherlands.